Highly Selective Room Temperature Monoreduction of Dinitro-arenes by Hydrogen Sulfide under Liquid–Liquid Biphasic Catalysis

UJJAL MONDAL, SUJIT SEN

Catalysis Research Laboratory, Department of Chemical Engineering, National Institute of Technology Rourkela, Rourkela, 769 008, India

Received 29 May 2017; revised 10 October 2017; accepted 10 October 2017

DOI 10.1002/kin.21136
Published online in Wiley Online Library (wileyonlinelibrary.com).

ABSTRACT: Selective reduction of one of the nitro group present in dinitro aromatic compounds by a novel Zinin reagent, H_2S-laden N-methyldiethanolamine (MDEA) solution, has been explored in the presence of tetra-*n*-butyl phosphonium bromide as a phase transfer catalyst under the liquid–liquid mode of reaction. Under the room temperature reaction condition, reduction of 2,4-dinitrotoluene (2,4-DNT) with H_2S-laden MDEA leads to the selective reduction of one nitro group present either at the fourth position to obtain 4-amino-2-nitrotoluene (4A2NT) or at the second position to get 2-amino-4-nitrotoluene (2A4NT). The reaction was very fast to achieve 100% conversion, and the selectivity of 4A2NT is much higher than the 2A4NT. A detailed parametric study was performed to analyze the effect of parameters on 2,4-DNT conversion and selectivity of both the isomers. The apparent activation energy was found to be as high as 46.25 kJ/mol, and the reaction was found to be kinetically controlled. An empirical kinetic model has been developed to correlate with the conversion version time data obtained experimentally. The present system dealt with an industrial problem in dealing with H_2S, present in by-product gaseous streams of many petroleum and natural gas industries. Novelties in the selective monoreduction lie in that fact that the reaction was done at room temperature

Correspondence to: Sujit Sen; e-mail: sensujit@nitrkl.ac.in.

Supporting Information is available in the online issue at www.wileyonlinelibrary.com.

(303 K), with a novel reagent, H_2S-laden MDEA solution. Therefore waste-minimization was effected to yield value-added fine chemicals, that is, amines. © 2017 Wiley Periodicals, Inc. Int J Chem Kinet 1–16, 2017

INTRODUCTION

Hydrogen sulfide (H_2S) gas is a major source of impurity in a gasification process of fossil fuels and found in many tail-gas streams of biogas plant, syngas production plant, and petrochemical plant [1,2]. H_2S gas is highly corrosive, toxic, and odorous in nature. H_2S concentration between 500 and 1000 ppm or more can be fatal for any living organism, and maximum allowable daily exposure limit without a significant chance of detrimental effects is only 1.4 ppb. It is very much obligatory to remove H_2S from gas streams as it can damage mechanical and electrical components of any control system and corrode energy generation and heat recovery units and pipelines [3,4]. The high content of sulfur in heavy crude oil generates a high amount of H_2S gas in downstream of petroleum and natural gas–processing industries. Strict environmental regulations have been imposed on the release of this by-product stream into the environment. This by-product gas stream is conventionally treated in an amine-treating unit (ATU) for the removal of H_2S gas, and then regenerated H_2S gas is oxidized in the Claus unit to produce elemental sulfur. The Claus process is facing the danger of extinction because of many reasons such as (i) underutilization of valuable hydrogen source, (ii) requirement of highly precise air rate control, (iii) the presence of trace sulfur compounds in the spent air, etc. Several reports can be found in the literature for the production of hydrogen and sulfur from H_2S gas, through thermal [5], photochemical [6], electrochemical [7–9], and thermochemical processes [10]. Syngas (H_2, CO), which has been reported to be produced by pyrolysis of acid gases (H_2S, CO_2), can be used as fuel for gas engines [11]. All the processes mentioned above are an arduous process with the expensive mode of operation and leads to excess production of elemental sulfur. Therefore, an economical, ecofriendly, and energy-saving process for better utilization of harmful H_2S gas is in high demand.

Nowadays, in the petroleum and natural gas industries, removal of sour gases containing H_2S and CO_2 is usually done by employing an aqueous solution of alkanolamines. Alkanolamines are most popular for sour gas absorption as they have less vapor pressure and can be used in a broad range of operating conditions (regarding temperature, pressure, concentration), and recyclable [12]. A copious amount of literature is available on the solubility study of acid gas mixture (CO_2 and H_2S) [13,14] or pure H_2S in diethanolamine or monoethanolamine solution [13–15]. H_2S gas can be selectively removed from the gases produced in refinery and coal gasification unit by an aqueous solution of *N*-methyldiethanolamine (MDEA) [16–19]. In the present study, aqueous MDEA solution is therefore utilized for selective absorption of H_2S as among all other alkanolamines tried in industries; MDEA has the minimum corrosion effect and causes a minute solvent loss due to its less vapor pressure, chemically stable, and economically viable.

Reduction of aromatic nitro compounds, with attached a multifunctional group on the aromatic ring, to aromatic amines, is a commercially important reaction. High-value chemical intermediates can be produced from aromatic amines, which are widely used as a raw material for many utility chemicals, like pharmaceuticals, fiber, explosives, polymers, cosmetics, pesticides, dyes, etc. [20–25]. Reduction of 2,4-dinitrotoluene (2,4-DNT) leads to the formation of 2-amino-4-nitrotoluene (2A4NT), 2-nitro-4-aminotoluene, and 2, 4-diaminotoluene. These products are industrially used as an intermediate for the production of dyes, artificial pigments [26,27].

Some commercially and academically well-known process for the reduction of nitroaromatic compounds are catalytic hydrogenation [28], Bechamp reduction [29], and Zinin reduction [30]. Reduction of dinitro aromatics like 2,4-DNT can give rise to a reduction of either both the nitro groups or a single nitro group selectively. In the reduction of 2,4-dinitrotoluene into 2,4-diaminotolune, several kinds of reagents have been tried out such as a Pd-pol catalyst in the presence of $NaBH_4$ [25], $Ni(OAc)_2{\cdot}4H_2O$ in the presence of $NaBH_4$ [31], and zinc in ammonium formate/HCOOH [32]. Hydrogen at different pressure levels has been employed in selective monoreduction of 2,4-DNT in the presence of various catalysts such as Pt/C [33], Au [34], and Ni-supported zeolite [35]. Hydrogenation of *p*-nitro-phenol has been carried out in the microbubble reaction system utilizing Pd/SN-ON(x) catalysts [36]. Yang et al. have observed 3 to10 fold of reaction rate of hydrogenation of a number of nitroarenes in the presence of Pt/C&PMO catalyst [37]. The Pickering emulsification technique has been used for the hydrogenation of *m*-nitrotoluene in the presence of solid catalyst (Pd/SM) [38]. The shortcomings

associated with all these processes are as follows: (1) extreme reaction conditions at the various level of process parameters, (2) tough process handling conditions and high safety concerns, (3) reduction of other functional groups present on the aromatic ring, (4) expensive mode of operation, and (5) undesired by-product formation. Monoreduction of polynitro-arenes can also be affected by negative divalent sulfur in the form of sulfide, hydrosulfide, and polysulfide and is called the Zinin reduction [39]. Many researchers employed ammonium sulfide or sodium sulfide as a source of sulfide and hydrosulfide ions in the Zinin reduction for reducing nitroaromatic compounds like chloronitrobenzene [38,40], nitrotoluene [17], nitroanisoles [41], 4-nitro-*o*-xylene [42], and 2,6-dinitrobenzoic acid [43]. Utilization of H_2S gas for the reduction of mononitroarenes has also been tried out [41,42], but the selective reduction of dinitro aromatic compounds by industrially important H_2S-laden MDEA has never been explored. In the present work, H_2S-laden MDEA is employed as a novel Zinin reagent for selective monoreduction in dinitro aromatics.

The current investigation uses a biphasic reaction system where the Zinin reagent, aqueous H_2S-laden MDEA forms the aqueous phase and the reactant dinitrotoluene, dissolved in solvent toluene, and forms the organic phase. To enhance the reaction rate between two immiscible phases, phase transfer catalysts (PTC) can be used. The reaction rate gets accelerated when PTC helps in transferring aqueous phase inorganic anions to the organic phase crossing the interface, and that promotes the reaction between organic reactants with the inorganic anions [44]. Biphasic reaction systems are of two types: liquid–solid and liquid–liquid (L–L) types [44–53]. The L–L PTC system (which is the case in the present study) is the most simple and widely accepted system, because of its several advantages such as operation simplicity, less requirement of solvent and raw materials compared to other processes, mild operating conditions, the higher selectivity of the product, and enhanced reaction rate.

Different types of PTCs have been used in multiphase reactions, like phosphonium salts, ammonium salts, crown ethers, cryptands, polyethylene glycols (PEG), etc. [47]. Quaternary phosphonium and ammonium salts are widely used among other PTCs for their higher reactivity, stability at a higher temperature, and less price. The quaternary phosphonium salts are more beneficial than the latter. The phosphonium cation is soft acid, and hydrosulfide anions (HS^-) are soft bases and as stated in Pearson's HSAB theory, transport of HS^- ions to the organic phase after binding with phosphonium cations is swifter than ammonium cation [52]. Ethyltriphenylphosphonium bromide (ETPPB), a quaternary phosphonium salt, was used in Zinin reduction, and the conversion achieved is comparable to the ammonium salt [40]. Tetra-*n*-butylphosphonium bromide (TBPB), another example of quaternary phosphonium salt, has been successfully employed as PTC in several different types of systems such as in the synthesis of alkyl and aryl thioglycoside and thiodisaccharide, in the one-pot synthesis of pyrano- and furanoquinolines, and in synthesis of *o*-nitrophenyl octyl ether [54–56]. For the above reasons, TBPB has been tried out as PTC in the current study, for selective reduction of dinitro aromatic compounds by H_2S-laden MDEA as a reducing agent at room temperature.

MATERIALS AND METHODS

Materials

2,4-DNT was purchased from Sigma-Aldrich (St. Louis, MO). TBPB was obtained from Sigma-Aldrich (Hong Kong, China), and potassium iodide (KI) and sodium hydroxide pellets (NaOH) were acquired from Rankem (New Delhi, India). Sodium thiosulfate pentahydrate ($Na_2S_2O_3{\cdot}5H_2O$) and toluene (≥99%) of analytical grade were obtained from Hi-Media (Mumbai, India). Starch soluble and sulfuric acid (≥98%) were acquired from Rankem (India). Potassium iodate (KIO_3), ferrous sulfide sticks (FeS), and MDEA (≥99%) of analytical grade were procured from Merck (Mumbai, India).

Experimental Setup and Procedure

For aqueous phase preparation, H_2S gas was bubbled through 35 wt% aqueous MDEA solution kept in an ice bath. The gas bubbling process was continued till desired sulfide concentration was attained. The sulfide concentration was determined by the iodometric titration method [57]. The main reaction was carried out in an isothermal baffled stirred batch reactor of 150 mL capacity in an inert nitrogen atmosphere. The reactor was provided with a digital speed regulation system and a PID temperature controller (±1°C). The reaction system consisted of an equal volume of the aqueous phase (H_2S-laden aqueous MDEA) and an organic phase (toluene used an organic solvent to dissolve 2,4-DNT) and a catalytic amount of quaternary phosphonium salt (TBPB). The aqueous phase was first introduced into the reactor followed by stirring the solution till the desired temperature was reached. After stopping the stirrer, the organic phase along with the TBPB was added into the reactor. The reaction commenced as soon as the stirrer was switched on again.

Table I Optimized Parameters for Each Experimental Run

Parameter (Unit)	Optimized Value	Range
Stirring speed (rpm)	1500	500–2500
Temperature (K)	303	303–328
Catalyst concentration (kmol/m^3)	0.0232	0–0.093
Reactant concentration (kmol/m^3)	0.549	0.2745–1.0981
Sulfide concentration (kmol/m^3)	2.5	1–2.5
MDEA concentration (kmol/m^3)	3.04	2.02–5.02
Volume of organic and aqueous phase (m^3)	3×10^{-5}	constant

0.1 mL of sample was collected from the upper organic phase layer after turning off the stirrer to allow the phase separation. Based on the earlier studies, range and optimized values of the operating parameters have been chosen to carry out the current Zinin reduction, and they are listed in Table I.

Method of Analysis

Samples withdrawn from the organic phase were analyzed by GC on an Agilent GC 7890B model. GC was fitted with a capillary column DB-5MS, 2 m × 3 mm, and nitrogen was used as a carrier gas at a flow rate of 1.6 cm^3/min. A flame ionization detector was used at a temperature of 573.15 K.

RESULTS AND DISCUSSION

Two products namely 4-amino-2-nitrotoluene (4A2NT) and 2A4NT were identified by GC-MS (Agilent 5977A model). No diamines or other products like nitroso or hydroxylamine derivative were found. So, the overall reaction can be written as follows:

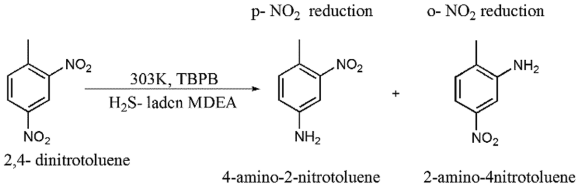

Proposed Mechanism of Reduction of 2,4-DNT under L–L PTC

As proposed by Zinin in 1842, the overall stoichiometry of the reduction reaction of nitroarenes by aqueous ammonium sulfide is given by Eq. (1) [39]. Sodium sulfide as a reducing agent for the reduction of aromatic nitro compounds also follows the same stoichiometry [39,40,57–59]:

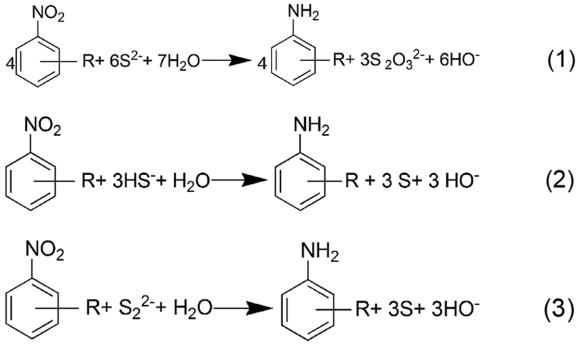

Elemental sulfur was found as a by-product of the reduction reaction of *p*-nitrophenylacetic acid with aqueous ammonium sulfide as shown in Eq. (2) [60]. Thiosulfate or elemental sulfur is generated as a by-product of two different reactions as shown in Eqs. (1) and (2). In the presence of a base, ammonia, the dissociation equilibrium favors toward more ionization [61] and as the concentration of ammonia increases the concentration of sulfide ions (S^{2-}) becomes more than that of hydrosulfide (HS^-) ions. Sodium disulfide was also used as the reducing agent, and the overall stoichiometry is shown in Eq. (3) [60]. Zinin reduction of 2,4-DNT with H_2S-laden MDEA is assumed to follow either Eq. (1) or (2).

Aqueous Phase Equilibrium. In the aqueous MDEA phase, sulfide (S^{2-}) and hydrosulfide (HS^-) ions exist in an ionic equilibrium, which is affected by the concentration of the MDEA [62]. The formation of both the anions is shown in Scheme 1 from Eqs. (4)–(6). Similar results were shown by ammonium sulfide solution [63].

Phase Transfer Catalysis in Biphasic L–L System. A general reaction mechanism of current reduction reaction has been proposed based on the current work and some previously published work (Scheme 1) [39,40,51,52]. Valency of sulfur can vary in a wide range (−2 to +6), and thus the presence of sulfur in different anionic forms (HS^-, HSO^-, HSO_2^-, HSO_3^-) in the reaction media is

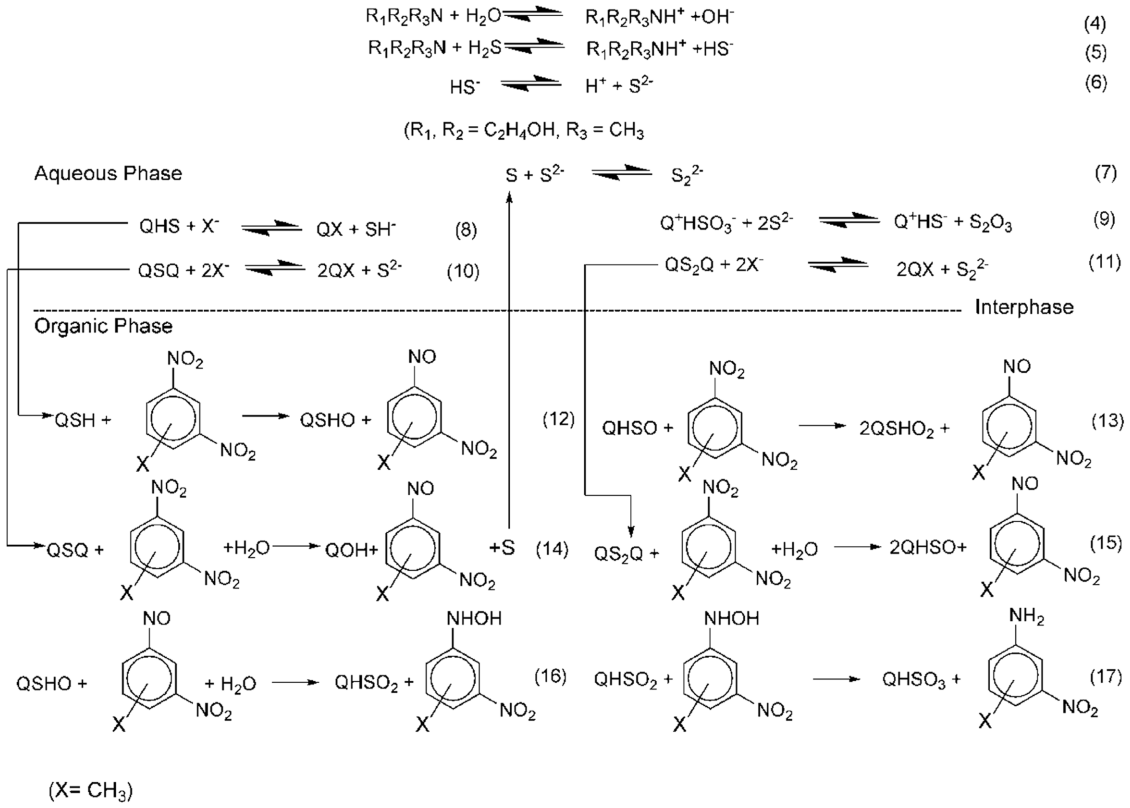

Scheme 1 Proposed mechanism of reduction of 2,4-DNT by H_2S-laden MDEA under L–L PTC.

very much possible and a proven fact. These anions can bind to a single quaternary cation very quickly [41].

The catalyst used for our study was TBPB, which is soluble in both the phases. The L–L PTC reaction pathway can be easily explained by Stark's extraction mechanism, according to which the PTC partitions into both phases. The catalyst cations present in the aqueous phase transfer the inorganic anions to the organic phase where it takes part in the reaction with the organic substrate.

The L–L PTC system is a cyclic process; it starts at the aqueous phase where quaternary cations (Q^+) rapidly pair with hydrosulfide ions (HS^-) to form Q^+ HS^- ion pair, and then the ion pair transfers to the organic phase. After that, it takes part in some complex elementary reaction as shown in Scheme 1 (Eqs. (12)–(17)). Without the presence of PTC, the similar reactions also occur, but it is rather a slow reaction. The end product of the reduction reaction of 2,4-DNT is 4-amino-4-nitrotoluene (4A2NT) and 2A4NT. The reduction reaction of the aromatic nitro compound to aromatic amines is an electron transfer reaction, which requires six electrons transfer through the formation of intermediates—nitrosobenzene and benzene hydroxylamines [61,62]. GC-MS analysis of the samples was not able to detect those intermediates, which may be due to the fast appearance and disappearance of those intermediates [35,39,40,61,63]. The selectivity of 2A4NT is less compared to 4A2NT. The reason is the nitro group present at the second position is sterically hindered by the methyl group present on the aromatic ring. So the reduction of nitro group present at the fourth position is easier than the second position, and as a result selectivity of 4A2NT is higher [35]. A few water molecules are also transferred to the organic phase along with the Q^+ HS^- ion pair and taking part in the reaction (Eqs. (14)–(16)). The quaternary ion pair gets inactivated ($Q^+HSO_3^-$) after the formation of the product (Eq. (17), and when it is transferred back to the aqueous phase it gets regenerated (Q^+ HS^-) after reacting with S^{2-} (Eq. (9)). The catalytic cycle continues when the reactivated ion pair is transferred back to the organic phase again.

The developed mechanism for the reduction of 2,4-DNT suggests that the Q^+ HS^- is the abundantly available ion pair among all other ions available in the aqueous phase. In the aqueous phase, eight reactions (Eqs. (4)–(11)) take place, and remaining reactions (Eqs. (12)–(17)) occur sequentially in the organic phase.

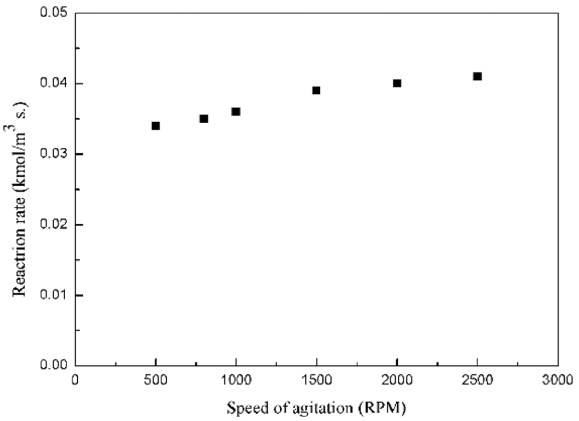

Figure 1 Effect of the stirring speed on the reaction rate. Temperature = 303 K, organic phase volume = 30 mL, concentration of 2,4-DNT in the organic phase = 0.549 M, concentration of TBPB = 0.0232 M, the aqueous phase volume = 30 mL, concentration of MDEA in the aqueous phase = 3.04 M, and concentration of sulfide in the aqueous phase = 2.5 M.

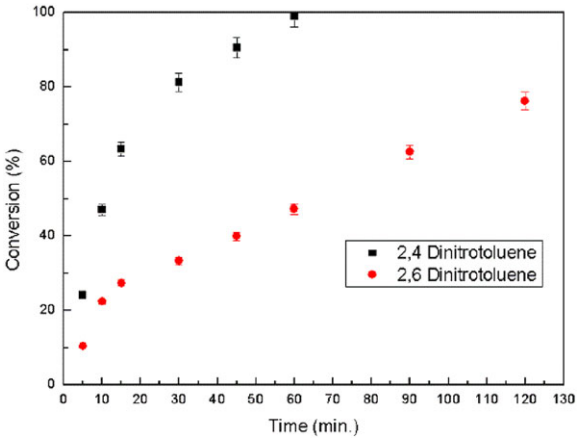

Figure 2 Conversion–time plot obtained experimentally of dinitrotoluenes. Stirring speed = 1500 rpm, temperature = 303 K, organic phase volume = 30 mL, concentration of reactant in the organic phase = 0.549 M, concentration of TBPB = 0.0232 M, aqueous phase volume = 3 mL, concentration of MDEA in the aqueous phase = 3.04 M, and concentration of sulfide in the aqueous phase = 2.5 M. [Color figure can be viewed at wileyonlinelibrary.com]

Parametric Studies

Effect of Agitation Intensity. The effect of the stirring speed on the reaction rate of 2,4-DNT disappearance in the L–L PTC system has been explored in the range of 500–2500 rpm in the presence of PTC. It is very clear from Fig. 1 that the variation of the initial reaction rate is very small due to change in the stirring speed. So it can be concluded that the reaction is kinetically controlled and free from any mass transfer resistance [41]. For elimination of the mass transfer effect, the stirring speed has been fixed at 1500 rpm during other parameter variation studies.

Comparison of Conversion between Different Dinitrotoluenes. In this study, the effectiveness of the developed reduction process by using H_2S-laden MDEA has been analyzed on different isomers of dinitrotoluenes, as shown in Fig. 2. For the current study, 2,4-DNT and 2,6-dinitrotoluene (2,6-DNT) have been used as a study material. From Fig. 2, it is very clear that reactivity of 2,4-DNT is higher than 2,6-DNT and 2,4-DNT was selectively reduced to 4A2NT (79.6%) and 2A4NT (20.4%). Reduction of 2,6-DNT results only 2-amino-6-nitrotoluene (2A6NT), and conversion achieved was 76.23% after 120 min of reaction. The nitro group present at the second and sixth positions that are sterically hindered by the methyl group attached to the aromatic ring. So, the reduction of nitro group present at the fourth position is swifter compared to the second and sixth positions. As a result, reactivity of 2,4-DNT was found of being higher than 2,6-DNT.

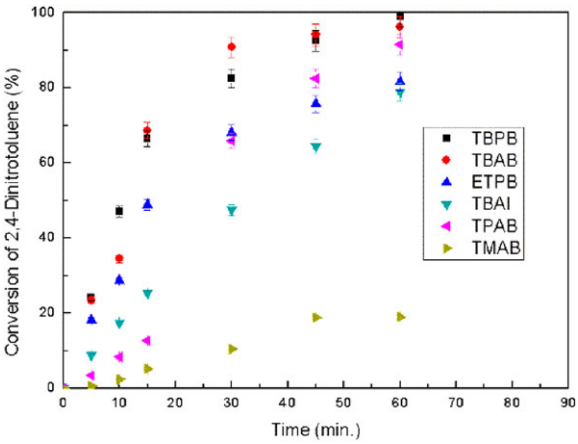

Figure 3 Effect of different catalysts on the conversion of 2,4-DNT. Stirring speed = 1500 rpm, temperature = 303 K, organic phase volume = 3 mL, concentration of 2,4-DNT in the organic phase = 0.549 M, concentration of TBPB = 0.0232 M, aqueous phase volume = 3 mL, concentration of MDEA in the aqueous phase = 3.04 M, and concentration of sulfide in the aqueous phase = 2.5 M. [Color figure can be viewed at wileyonlinelibrary.com]

Effect of Different Phase Transfer Catalysts. The selective reduction of 2,4-DNT was studied with different PTC as shown in Fig. 3. Catalysts taken for the comparison studies are tetrabutylammonium bromide (TBAB), tetrabutylphosphonium bromide (TBPB), tetramethylammonium bromide (TMAB),

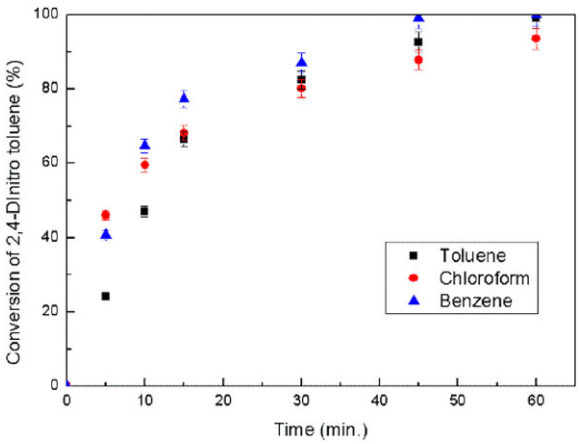

Figure 4 Effect of different solvents on the conversion of 2,4-DNT. Stirring speed = 1500 rpm, temperature = 303 K, organic phase volume = 30 mL, concentration of 2,4-DNT in the organic phase = 0.549 M, concentration of TBPB = 0.0232 M, aqueous phase volume = 30 mL, concentration of MDEA in the aqueous phase = 3.04 M, and concentration of sulfide in the aqueous phase = 2.5 M. [Color figure can be viewed at wileyonlinelibrary.com]

tetrabutylammonium iodide (TBAI), ETPPB, and tetrapropylammonium bromide (TPAB). The order of the reactivity of these catalysts is TBPB > TBAB > TPAB > ETPB > TBAI > TMAB. With a higher number of carbon atom in the alkyl group of PTC, the lipophilicity and extraction rate of PTC enhances, which in turn generates higher productivity. ETPPB is having a higher carbon number although it is showing less reactivity than other ammonium and phosphonium salts (TBPB, TBAB, and TPAB). As the only single methyl group and three big benzyl group are attached to the quaternary cation in ETPPB, the quaternary cation is not easily accessible for anions, and the reaction rate gets slower. The phosphonium salt (TBPB) has shown better reactivity than ammonium salts (TBAB, TBAI).

Effect of Other Organic Solvents. In this study, most common organic solvents such as chloroform, benzene, and toluene were employed to analyze the effect of their polarities (dielectric constant) on the reactivity of the reduction reaction as shown in Fig. 4. According to the Stark's mechanism, PTC must transfer the reactive anions into the organic phase to react with the organic substrate. If the reactive anions are firmly held by a cation, the reaction rate will be hindered. Strong solvation (including hydration) of the anions in the solvent also affects the reactivity. Nonpolar solvents promote higher reactivity by reducing the extent of solvation of anions and by increasing the concentration of PTC in the organic phase. But if the polarity of the solvent is low then the catalyst is unable to ionize, and hence reactivity will be very low, and the distribution of the catalyst in both the phases is also affected by the solvent [64]. The maximum deviation in the conversion of 2,4-DNT was found to be 7% because of the change of a solvent. So, the effect of solvent is not significant, and therefore the solvent effect can be ignored. Therefore, in kinetic modeling, we did not consider the solvent effect. The dielectric constant of the solvents used is in order of chloroform > benzene > toluene. And the conversion (and reactivity) of 2,4-DNT in the solvents follows the following order: benzene > toluene > chloroform. Thus, in the current reaction system, toluene has been used as an effective solvent. Like in our present case, toluene was also found to be a better solvent in other biphasic phase transfer catalytic reaction systems [65].

Effect of Temperature of the Reaction. To study the effect of temperature on the conversion of 2,4-DNT in the L–L PTC system, the temperature of the reaction was varied in the range of 313–343K and rest of all reaction conditions were kept constant (Fig. 5a). From the theory of transition state, the rate of a reaction increases with the rise in temperature because increasing temperature provides the energy required to overcome the reaction barrier. It is evident from the figure that the temperature variation has a great impact on reactivity (conversion) of 2,4-DNT. With increasing temperature, the collision between reactant molecules is becoming more frequent and thus the reaction rate gets enhanced.

The initial rates at different temperatures were determined, and the Arrhenius plot of ln (initial rate) 2,6-DNT versus $1/T$ is drawn (Fig. 6). The slope of the best fitted straight line gives us apparent activation energy as 46.25 kJ/mol. As the value of the apparent activation energy is high, the reaction is kinetically controlled. The activation energy of the same order of magnitude has been obtained in the selective reduction of other nitro compounds, and it was also proposed to be kinetically controlled one [39,60]. As the conversion reached 100% after 60 min of reaction for each temperature study, a selectivity plot (Fig. 5b) is drawn based on the data of 30 min of reaction. The selectivity of the two isomers of aminonitrotoluene follows different trends with increasing temperature, although there was an enhancement of the overall conversion of 2,4-DNT. From the plot (Fig. 5c), it is clear that with increasing temperature the selectivity of 4A2NT has decreased.

Effect of Catalyst Concentration. To study the effect of the catalyst concentration, at five different catalyst concentrations (0–0.093 M), the conversion of 2,4-DNT was determined and is shown in Fig. 7a. The

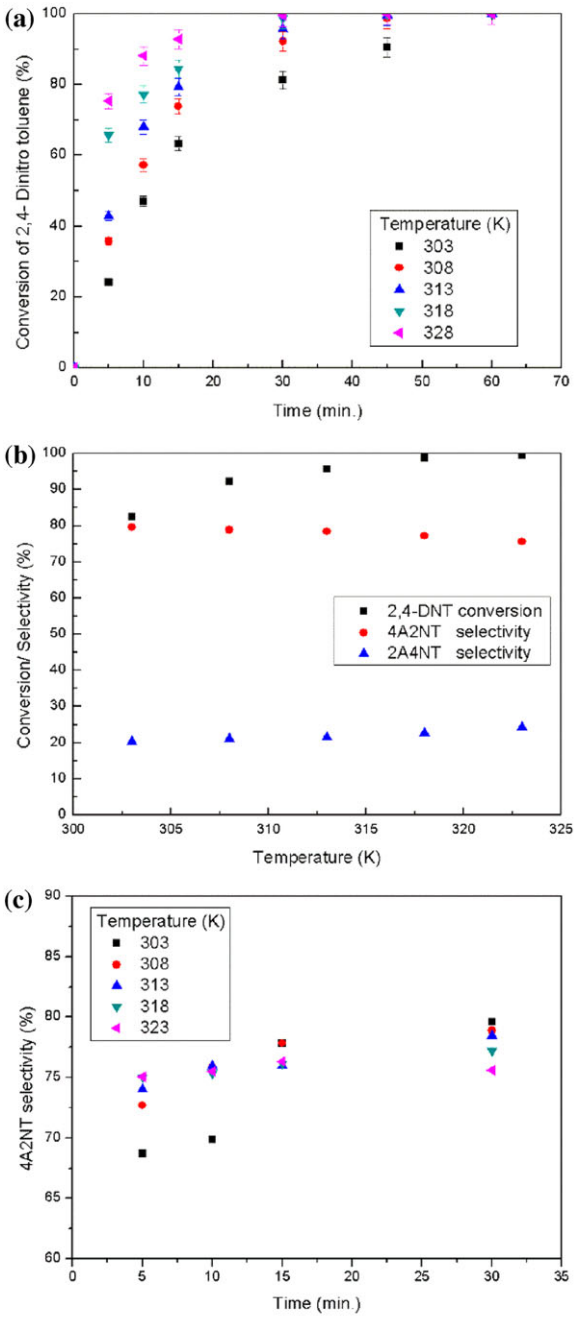

Figure 5 Effect of temperature on (a) the conversion of 2,4-DNT, (b) the selectivity of 4A2NT and 2A4NT with respect to temperature, and (c) the selectivity of 4A2NT with respect to reaction time. Stirring speed = 1500 rpm, organic phase volume = 30 mL, concentration of 2,4-DNT in the organic phase = 0.549 M, concentration of TBPB = 0.0232 M, aqueous phase volume = 30 mL, concentration of MDEA in the aqueous phase = 3.04 M, and concentration of sulfide in the aqueous phase = 2.5 M. [Color figure can be viewed at wileyonlinelibrary.com]

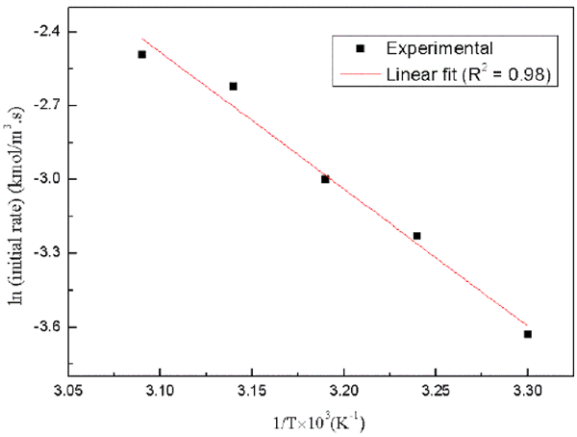

Figure 6 Arrhenius plot of ln (initial reaction rate) versus 1/*T*. All other conditions are same as in Fig. 5. [Color figure can be viewed at wileyonlinelibrary.com]

conversion of 2,4-DNT, as well as the reaction rate, enhances when the catalyst concentration increases. Reactant conversion was found to be 100% with 0.0232 M of catalyst loading, whereas it was about 70% without catalyst after 60 min of reaction. The highest enhancement factor of 5.2 was achieved with the catalyst concentration of 0.093 M, as shown in Table II. The influence of catalyst loading on the selectivity of 4A2NT and 2A4NT is shown in Fig. 7b after 30 min of reaction. From Fig. 7c, it is evident that with the catalyst concentration of 0.0465 M, the highest selectivity of 4A2NT was attained and with further catalyst loading the selectivity of 4A2NT has been found to decrease gradually.

To determine the order of reaction with respect to the catalyst concentration, the initial reaction rate was calculated at different catalyst concentrations. A plot of ln (initial rate) against ln (catalyst concentration) was made and is shown in Fig. 8. From the slope of the linear fit line, the order of reaction was determined. The order of the reaction was found out to be 0.64 with respect to the TBPB concentration.

Effect of the 2,4-DNT Concentration. The influence of the concentration of 2,4-DNT, on the kinetics of the reaction, was studied in the concentration range of 0.2745–1.0981 kmol/m^3 and is presented in Fig. 9a. It can be understood from the figure that with the increase of the concentration of 2,4-DNT, the conversion of 2,4-DNT has reduced. The selectivities of 4A2NT and 2N4AT found at different concentrations of 2,4-DNT are shown in Fig. 9b. According to Fig. 9c, the selectivity of 4A2NT is increasing gradually with the increase in the concentration of 2,4-DNT. At the highest concentration of 1.0981 M of reactant, the selectivity

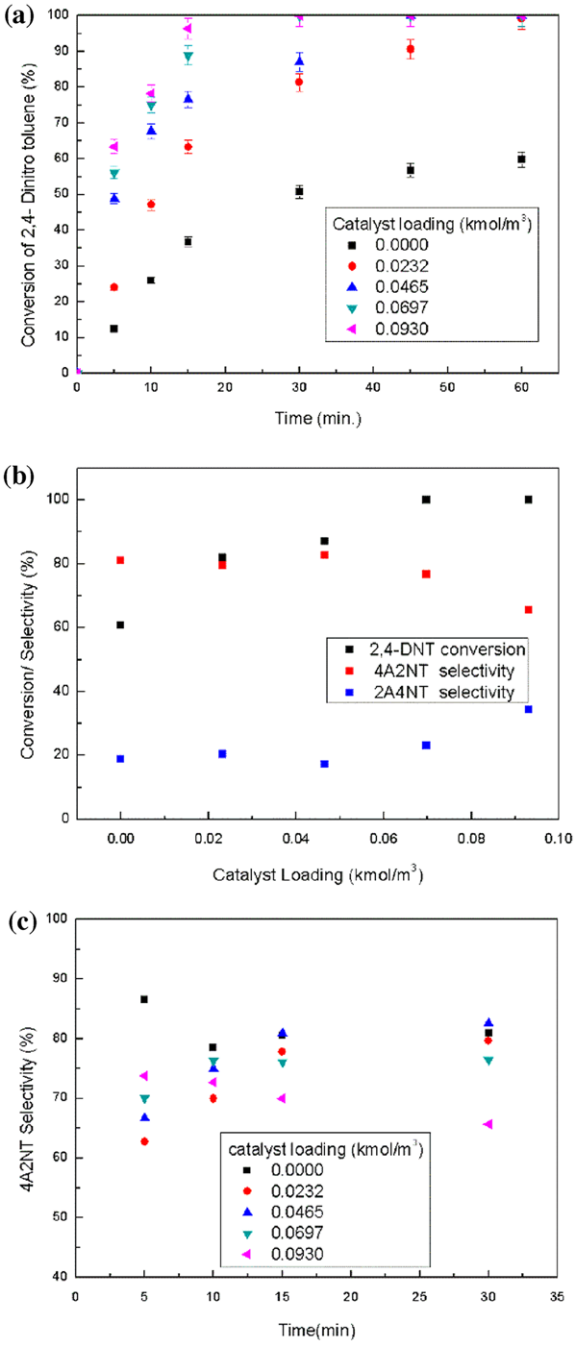

Figure 7 Effect of the TBPB concentration on (a) the conversion of 2,4-DNT, (b) the selectivity of 4A2NT and 2A4NT with respect to catalyst loading, and (c) the selectivity of 4A2NT with respect to reaction time. Stirring speed = 1500 rpm, temperature = 303 K, organic phase volume = 30 mL, concentration of 2,4-DNT in the organic phase = 0.549 M, concentration of TBPB = 0.0232 M, aqueous phase volume = 30 mL, concentration of MDEA in the aqueous phase = 3.04 M, and concentration of sulfide in the aqueous phase = 2.5 M. [Color figure can be viewed at wileyonlinelibrary.com]

Table II Effect of the Catalyst Concentration on the Initial Reaction Rate

TBPB Concentration (kmol/m^3 of Organic Phase)	Initial Reaction Rate (kmol/m^{3}s)	Enhancement Factor
0.0000	0.0136	1.0
0.0232	0.0264	2.0
0.0465	0.0536	3.0
0.0697	0.0613	4.5
0.0930	0.0696	5.2

All other conditions are same as in Fig. 7.

of 4A2NT was 82.26%. From Fig. 10, the order of reaction with respect to the 2,4-DNT concentration was obtained as 0.47.

Effect of Concentration of Sulfide Ion in the Aqueous Phase. The conversion of 2,4-DNT is greatly influenced by the sulfide ions concentration in the aqueous phase as shown in Fig. 11a. For this study, the sulfide concentration in the aqueous phase was varied in the range of 1.0–2.5 M. As the concentration of sulfide increases, the conversion of 2,4-DNT also gets enhanced. Figure 11b shows how the selectivity of 4A2NT is affected by the change in the sulfide concentration, and it is found from Fig. 11c that with a higher concentration of sulfide selectivity of 4A2NT is gradually decreased. From the plot of ln (initial rate) against ln (sulfide concentration) (Fig. 12), the slope of the linear fit line is found to be 1.93.

Effect of MDEA Concentration. There is no direct influence of the MDEA concentration on the reaction kinetics, but it still affects the chemical equilibria of the MDEA–H_2O–H_2S system. As shown in Scheme 1,

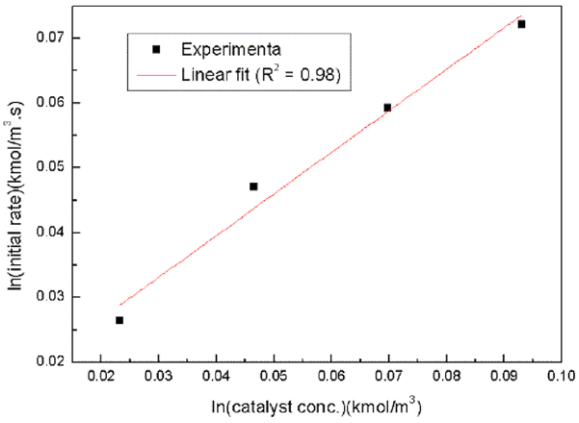

Figure 8 Plot of ln (initial reaction rate) versus ln (catalyst concentration). All other conditions are same as in Fig. 7. [Color figure can be viewed at wileyonlinelibrary.com]

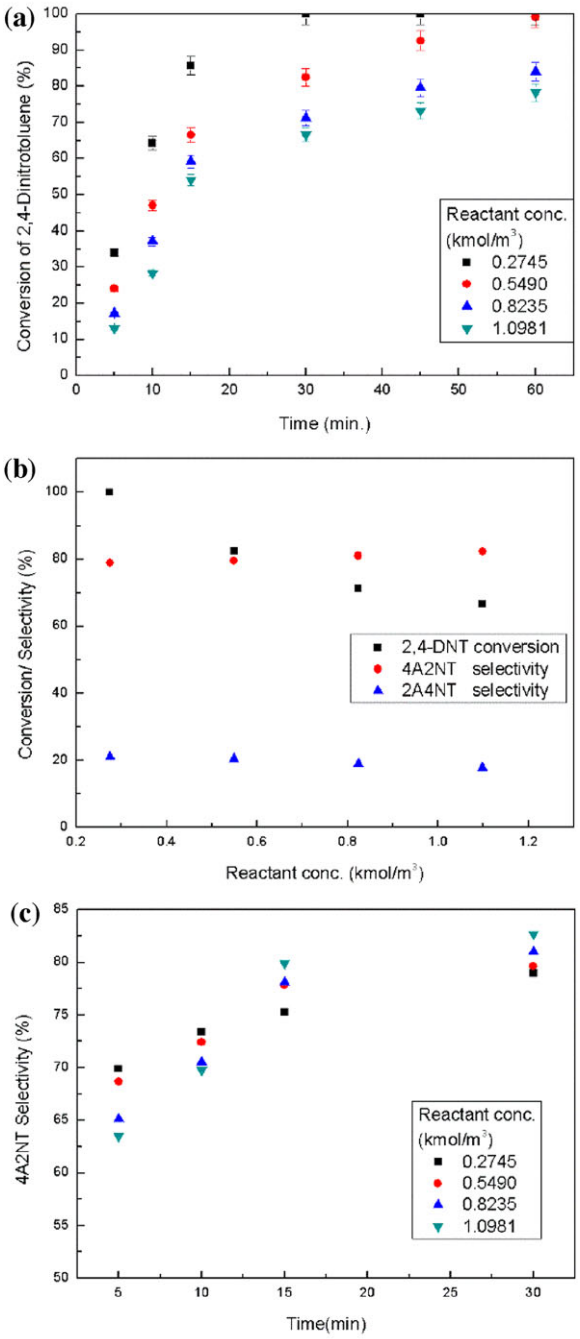

Figure 9 Effect of the 2,4-DNT concentration on (a) the conversion of 2,4-DNT, (b) the selectivity of 4A2NT and 2A4NT with respect to the reactant concentration, and (c) the selectivity of 4A2NT with respect to reaction time. Stirring speed = 1500 rpm, temperature = 303 K, organic phase volume = 30 mL, concentration of TBPB = 0.0232 M, aqueous phase volume = 30 mL, concentration of MDEA in the aqueous phase = 3.04 M, and concentration of sulfide in the aqueous phase = 2.5 M. [Color figure can be viewed at wileyonlinelibrary.com]

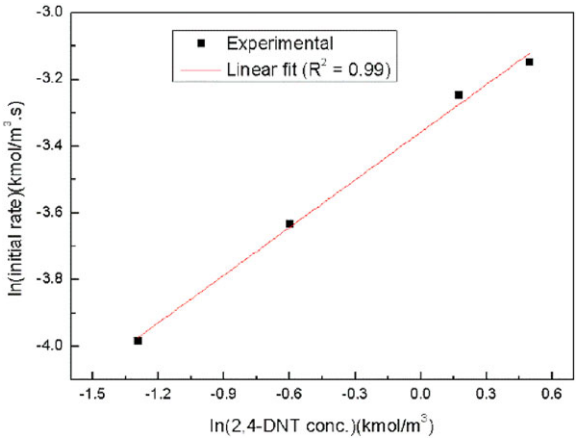

Figure 10 Plot of ln (initial rate) versus ln (2,4-DNT). All other conditions are same as in Fig. 9. [Color figure can be viewed at wileyonlinelibrary.com]

active anions like sulfide (S^{2-}) and hydrosulfide (HS^-) are formed in the aqueous phase and both the active anions take part in the reactions as shown in Eqs. (1) and (2). Owing to the basic nature of MDEA, ionization of H_2S in the aqueous phase is easier and availability of sulfide ions (S^{2-}) is more than hydrosulfide ions (HS^-). MDEA variation with a fixed sulfide concentration can give some idea about the existence of both the reactions.

The color of the aqueous solution changes from greenish yellow to orange and then finally to reddish brown during the whole process of the reaction, and this phenomenon indicates the progress of the reaction. The reddish brown color is due to the formation of polysulfide ions, which came into existence as the reaction proceeds further [66].

In the present study, after 60 min of run time, 87.34% conversion of 2,4-DNT was achieved with the highest MDEA concentration of 5.02 M with a sulfide concentration 1.37 M in the aqueous phase, as shown in Fig. 13a. These results support that the reaction follows Eq. (1). Similar observations were found when scientists used aqueous ammonium sulfide solution for the reduction of nitroaromatic compounds [39,58]. The highest conversion achieved during MDEA variation was 87.34%, and the current result is much higher than the conversion obtained according to Eq. (1) (approximately 60%) or Eq. (2) (approximately 30%). It can be explained by assuming that the reaction either follows both Eq. (1) and (2) or it follows Eq. (3). As reaction proceeds, polysulfide ions formed (as color intensifies to red), when sulfide ions react with elemental sulfur (produced in Eq. (2)), and higher conversion can be achieved.

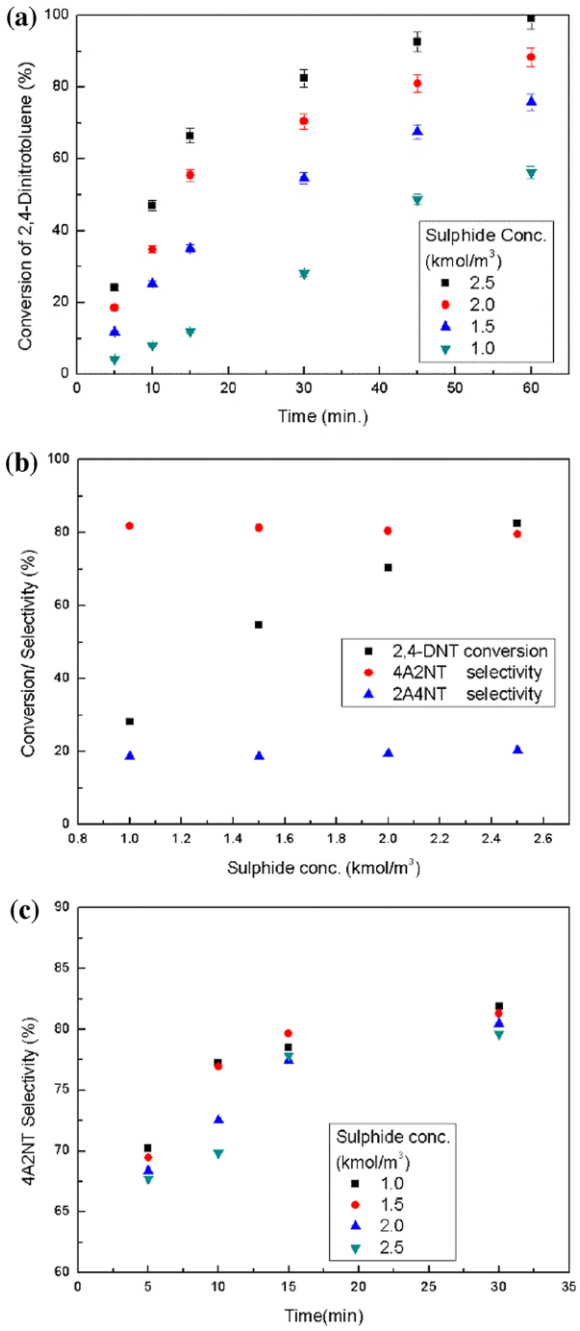

Figure 11 Effect of the sulfide concentration on (a) the conversion of 2,4-DNT, (b) the selectivity of 4A2NT and 2A4NT with respect to the sulfide concentration, and (c) the selectivity of 4A2NT with respect to reaction time. Stirring speed = 1500 rpm, temperature = 303 K, organic phase volume = 30 mL, concentration of 2,4-DNT in the organic phase = 0.549 M, concentration of TBPB = 0.0232 M, aqueous phase volume = 30 mL, concentration of MDEA in the aqueous phase = 3.04 M, and concentration of sulfide in the aqueous phase = 2.5 M. [Color figure can be viewed at wileyonlinelibrary.com]

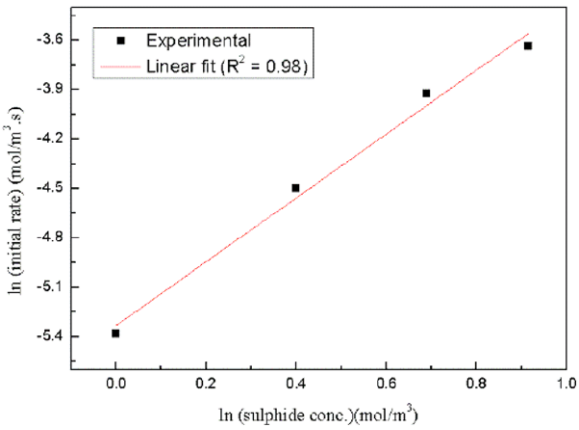

Figure 12 Plot of ln (initial rate) versus ln (sulfide concentration). All other conditions are same as in Fig. 11. [Color figure can be viewed at wileyonlinelibrary.com]

So it can be concluded that the increase in the MDEA concentration with the fixed sulfide concentration enhances the number of sulfide ions, and that enhances the conversion of 2,4-DNT. Figures 13b and 13c show the effect of the MDEA concentration on the selectivity of 4A2NT. From the figure, it is clear that there is a slender influence of the MDEA concentration on the selectivity of either 4A2NT or 2A4NT. With increasing MDEA concentration from 2.02 to 5.02 M, the conversion of 2,4-DNT increases but the selectivity of 4A2NT decreases slightly from 82.5% to 80.2%.

Effect of Elemental Sulfur Loading. Owing to addition of sulfur powder, a change in the color of H_2S-laden MDEA solution was observed from dark green to orange. A similar phenomenon of color change was noticed during MDEA variation. The effect of sulfur powder loading on the reactivity of 2,4-DNT is shown in Fig. 14, and the "S" nature of the curve can be observed. An initial hike in the reaction rate is noted in the figure because of the addition of elemental sulfur, but as the reaction proceeds the reaction rate became slower. It can be assumed that polysulfide ions (S_n^{2-}, where $2 \leq n \leq 6$) were formed, among which disulfide ions were in majority (Eq. (7)); these ions can easily be transferred to the organic phase in comparison with sulfide (S^{2-}), hydrosulfide (HS^-), and other polysulfide ions (S_n^{2-}, where $3 \leq n \leq 6$). The reduction rate of 2,4-DNT with disulfide ions is faster [67]. It is an established fact that polysulfide is a selective reducing agent for nitro reduction [66]. Conversion of 2,4-DNT in the run without elemental sulfur addition became higher after 15 min of reaction. The sole reason for this crossover may be the formation of elemental sulfur as the reaction proceeds (Eq. (2)). The sharp rise in the conversion of reactant for no sulfur addition case

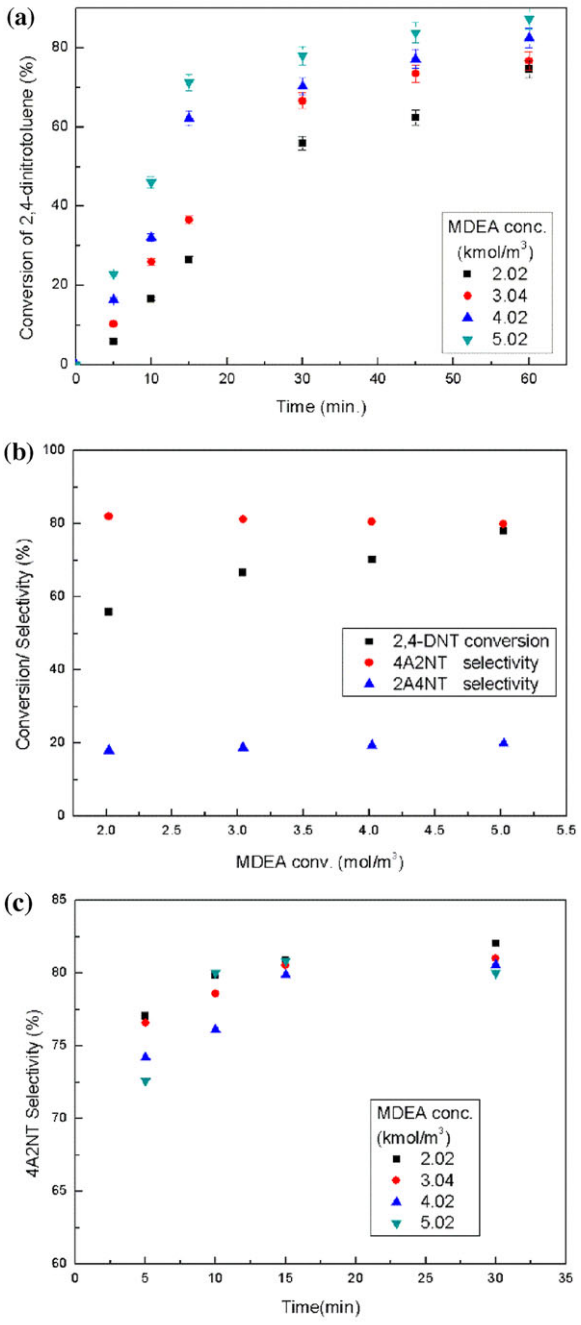

Figure 13 Effect of the MDEA concentration on (a) the conversion of 2,4-DNT, (b) the selectivity of 4A2NT and 2A4NT with respect to the MDEA concentration, and (c) the selectivity of 4A2NT with respect to reaction time. Stirring speed = 1500 rpm, temperature = 303 K, organic phase volume = 30 mL, concentration of 2,4-DNT in the organic phase = 0.549 M, concentration of TBPB = 0.0232 M, aqueous phase volume = 30 mL, and concentration of sulfide in the aqueous phase = 2.5 M. [Color figure can be viewed at wileyonlinelibrary.com]

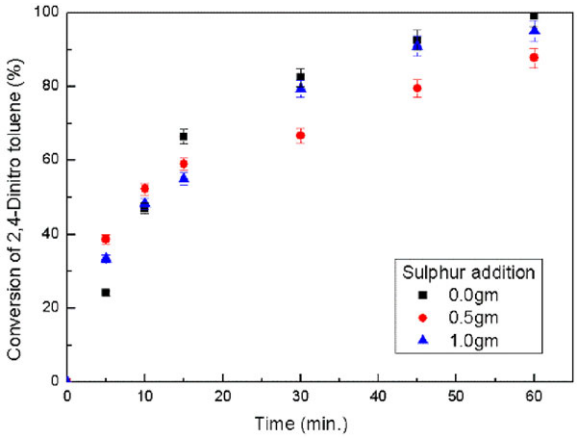

Figure 14 Effect of elemental sulfur addition on the conversion of 2,4-DNT. Stirring speed = 1500 rpm, temperature = 303 K, organic phase volume = 30 mL, concentration of 2,4-DNT in the organic phase = 0.549 M, concentration of TBPB = 0.0232 M, aqueous phase volume = 30 mL, concentration of sulfide in the aqueous phase = 2.5 M, and concentration of MDEA in the aqueous phase = 3.04 M. [Color figure can be viewed at wileyonlinelibrary.com]

is due to the in situ production of elemental sulfur and consequent production of disulfide and other polysulfides that enhance the reduction process.

Kinetic Modeling of L–L PTC

A kinetic model has been developed based on the proposed mechanism shown in Scheme 1. The reaction occurring at interphase between the aqueous and organic phases is also contributing significantly to the overall reaction. From Fig. 7a the without catalyst run shows 70% conversion.

It is further assumed that the overall L–L PTC reaction follows both Eqs. (1) and (2) where 2,4-DNT present in the organic phase is selectively reduced by sulfide and hydrosulfide anions present in the aqueous phase to yield 4A2NT and 2A4NT as the main products.

To eliminate the mass transfer effect, the reaction mixture was agitated with at an optimum stirring speed of 1500 rpm. As the reaction commences, the PTC catalyst ion-pair $Q^+ X^-$ ($X^- = Cl^-$) exchanges its anions with HS^- ions very rapidly in the aqueous phase to transform into active catalyst ion pair ($Q^+ HS^-$). The active catalyst ion pair is then transferred to the organic phase crossing the interface. After that the reaction proceeds in the organic phase, and different transition anions are formed. Finally, the active catalyst became inactive as the HSO_3^- ion gets attached to quaternary

cations Q^+. Q^+ HSO_3^- ions are transferred to the aqueous phase and react with S^{2-} to get reactivated as Q^+ HS^- again.

The elemental sulfur produced in the reaction is enhancing the reaction rate initially, and it is the reason for the "S" nature of the conversion versus time curve (Fig. 14). The formation of polysulfide occurs when elemental sulfur reacts with H_2S-laden MDEA solution. Previously, it was discussed that the overall conversion is decreased with the addition of elemental sulfur due to the formation of polysulfide in a large number in comparison with disulfide ions, in which the catalyst cation cannot be transferred easily to the organic phase. According to Eq. (3), the disulfide (S^{2-}) ions form ion pair with two catalyst cations (Q^+ $S^{2-}Q^+$) in the aqueous phase and transfer to the organic phase.

Development of a mathematical model based on the mechanism proposed is quite difficult because of the complexities involved in the current reaction as the selective reaction of dinitro compound gives us two products, that is, 4A2NT and 2A4NT. So in our current study, an empirical kinetic model has been developed to correlate with the conversion version time data obtained experimentally. In our current study, the reaction order with respect to catalyst, reactant, and sulfide concentration has been evaluated and based on these the rate of the reduction reaction of 2,4-DNT ($-r_R$) is expressed by Eq. (18)

$$-r_R = k_1 C_R^{0.47} C_S^{1.93} C_C^{0.64} + k_2 C_R^{0.47} C_S^{1.93} C_C^{0.64} C_E \tag{18}$$

where C_R and C_c are the concentration of 2,4-DNT and catalyst (TBPB) in the aqueous phase. Owing to the formation of elemental sulfur in a reaction medium, the curve is of "S" nature and it is defined by the second term of the reaction rate (Eq. (18)). The concentration of sulfide (C_S) and elemental sulfur (C_E) in the aqueous phase is derived from the overall mass balance based on the stoichiometry of Eq. (2), and these are shown in the following expressions:

$$C_S = C_{SO} - 3f\,(C_{RO} - C_R) \tag{19}$$

$$C_E = f\,(C_{RO} - C_R) \tag{20}$$

where C_{SO} and C_{RO} are the concentration of the initial sulfide concentration in the aqueous phase and 2,4-DNT concentration added in the organic phase, f is the volume ratio between the organic and aqueous phase and parameter estimation is done by a nonlinear regression algorithm. The optimum values of the rate constants k_1 and k_2 were calculated at different temperatures by minimizing the objective function (E) as given by the following equation:

$$E = \sum_{i=1}^{n} \left[\{(-r)_{\text{pred}}\}_i - \{(-r)_{\text{expt}}\}_i\right]^2 \tag{21}$$

In Table III, the calculated values of k_1 and k_2 are listed. From the slope of the Arrhenius plots shown in Figs. 15a and 15b, the activation energies are calculated for both rate constants (k_1 and k_2) and it is 75.65 and 48.72, respectively.

Table III Rate Constants of the Model

Temperature (K)	$k_1 \times 10^{-4}$ $((\text{kmol/m}^3)^{-3.04}\ \text{s}^{-1})$	$k_2 \times 10^{-4}$ $((\text{kmol/m}^3)^{-4.04}\ \text{s}^{-1})$
303	7.10	15.80
308	13.60	11.82
313	22.42	9.02
318	30.27	6.11

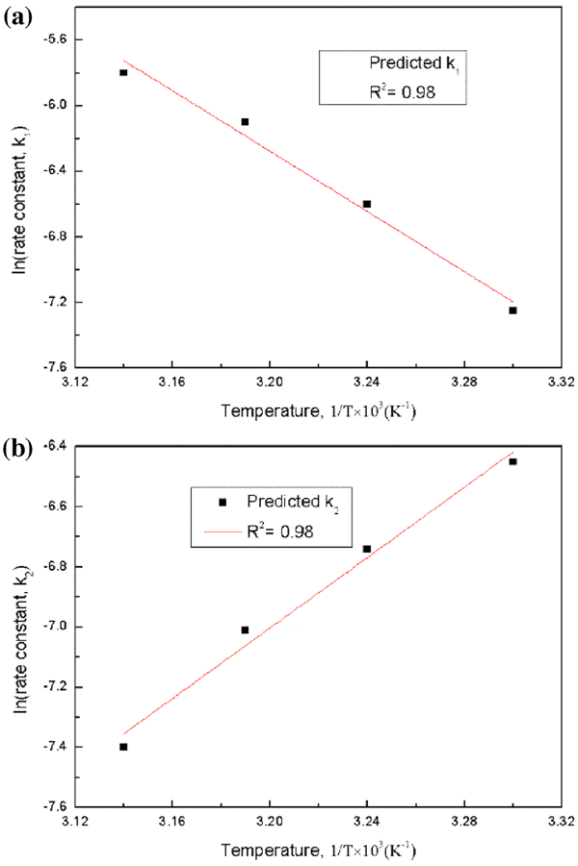

Figure 15 Arrhenius plot of (a) ln (rate constant, k_1) versus $1/T$ and (b) ln (rate constant, k_2) versus $1/T$. [Color figure can be viewed at wileyonlinelibrary.com]

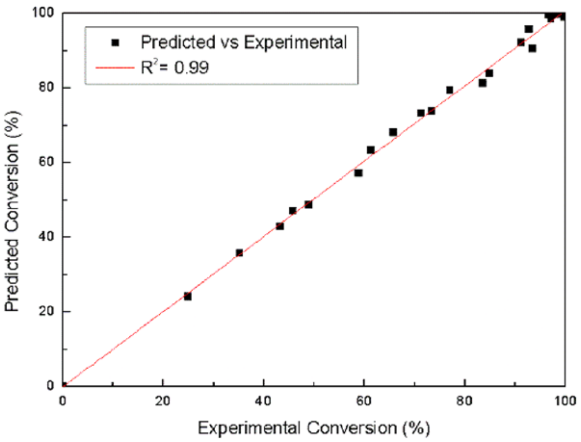

Figure 16 Comparison between calculated conversion and experimental conversion of 2,4-DNT at different temperatures after 60 min of reaction. [Color figure can be viewed at wileyonlinelibrary.com]

Kinetic Model Validation

From the regression model, the predicted reaction rate is evaluated and based on the predicted rates a comparison study between the predicted conversion versus experimental conversion is plotted in Fig. 16. Excellent agreement was observed between the predicted and experimental conversion.

CONCLUSIONS

The current study shows the novelties of L–L PTC in the selective reduction of 2,4-DNT to the corresponding amino compound by the novel Zinin reagent, H_2S-laden MDEA under milder reaction conditions, thereby eliminating the use of a costly metallic catalyst, high-temperature, and high-pressure reaction. As the reaction was very fast, 100% conversion was achieved in a very short time at room temperature (303 K). Selective reduction leads to the formation of two mononitro amine isomers: 2A4NT and 4A2NT. Selectivity of 4A2NT was found to be higher than 2A4NT. The detailed parametric study suggested that with the increase of temperature, catalyst concentration, sulfide ion concentration, MDEA concentration, the selectivity of 4A2NT decreases and that of 2A4NT increases. The highest selectivity of 4A2NT was observed as 82.26% when the reactant concentration in the reactor was 1.0981 kmol/m^3. A suitable reaction mechanism has been proposed, and a kinetic model has been developed based on the mechanism. The kinetic model based on the first-order approximation has been successfully validated against the experimental data. The activation energy was found to be 46.25 kJ/mol from experimental findings.

Dr. Mondal is thankful for a doctoral fellowship from Ministry of Human Resource and Development (MHRD), India during the tenure of the work.

NOMENCLATURE

C^{aq}_{QX}	QX concentration in the aqueous phase, kmol/m^3
C^{org}_{QX}	QX concentration in the organic phase, kmol/m^3
C^{org}_{QHS}	QHS concentration in the organic phase, kmol/m^3
C^{aq}_{QHS}	QHS concentration (also $[Q^+\ HS^-]_a$) in the aqueous phase, kmol/m^3
C^{aq}_{QSQ}	QSQ concentration in the aqueous phase, kmol/m^3
C^{org}_{QSQ}	QSQ concentration in the organic phase, kmol/m^3
$C^{aq}_{QS_2Q}$	QS_2Q concentration in the aqueous phase, kmol/m^3
$C^{org}_{QSHO_3}$	$QSHO_3$ concentration (also $Q^+SHO_3^-$) in the aqueous phase, kmol/m^3
$C^{aq}_{QSHO_3}$	$QSHO_3$ concentration in the aqueous phase, kmol/m^3
$C^{aq}_{S_2O_3}$	$S_2O_3{}^{2-}$ concentration in the aqueous phase, kmol/m^3
$C^{aq}_{S^2}$	$[S^{2-}]^2$ concentration in the aqueous phase, kmol/m^3
$C^{org}_{ArNO_2}$	$ArNO_2$ concentration in the organic phase, kmol/m^3
C^{*}_{QX}	Catalyst (QX) concentration initially fed to the aqueous phase, kmol/m^3
C_{Q^T}	Total catalyst Q concentration in the organic phase, kmol/m^3
$C^{*}_{ArNO_2}$	Total reagent ($ArNO_2$) concentration added in the organic phase, kmol/m^3
$K_1 = \frac{C^{aq}_{QSHO_3}}{C^{org}_{QSHO_3}}$	
$K_2 = \frac{k_1}{k_1'} = \frac{C^{aq}_{QHSO_3}\ C^{aq}_{S_2O_3}}{C^{aq}_{QHSO_3}\ C^{aq}_{S^2}}$	$C^{org}_{QS_2Q}$
K_3	$\frac{C^{aq}_{QX}}{C^{org}_{QX}}$

K_4	$\frac{C^{org}_{QHS}}{C^{aq}_{HS}}$
K_5	$\frac{C^{org}_{QSQ}}{C^{oq}_{QSQ}}$
K_6	$\frac{C^{org}_{QS_2Q}}{C^{aq}_{QS_2Q}}$
K_{app}	Apparent first-order reaction rate constant, m^3/(mol of catalyst·min)
k_1	Forward reaction rate constant [m^3/(mol of catalyst·min)] aqueous phase
k_1'	Backward reaction rate constant [m^3/(mol of catalyst·min)] aqueous phase
k_2	Reaction rate constant [m^3/(mol of catalyst·min)] organic phase
k_3	Reaction rate constant [m^3/(mol of catalyst·min)] organic phase
k_3	Reaction rate constant [m^3/(mol of catalyst·min)] organic phase
V^o	Volume of organic phase, m^3
V^a	Volume of the aqueous phase, m^3
X	Fractional conversion
t	Time, min

BIBLIOGRAPHY

1. Belmabkhout, Y.; De Weireld, G.; Sayari, A. Langmuir 2009, 25, 13275–13278.
2. Koyuncu, D. D. E.; Yasyerli, S. Ind Eng Chem Res 2009, 48, 5223–5229.
3. Polychronopoulou, K.; Fierro, J. L. G.; Efstathiou, A. M. Appl Catal B Environ 2005, 57, 125–137.
4. Rezaei, S; Tavana, A.; Sawada, J. A.; AWu, L.; Junaid, A. S. M.; Kuznicki, S. M. Ind Eng Chem Res 2012, 51, 12430–12434.
5. Faraji, F; Safarik, I.; Strausz, O. P.; Yildirim, E. M.; Torres, E. Int J Hydrogen Energy 1998, 23, 451–456.
6. Cervera-March, S.; Borrell, L.; Giménez, J.; Simarro, R.; Andojar, J. M. Int J Hydrogen Energy 1992, 17, 683–688.
7. Huang, H.; Yu, Y.; Chung, K. H. Energy Fuels 2009, 23, 4420–4425.
8. Petrov, K.; Srinivasan, S. Int J Hydrogen Energy 1996, 21, 163–169.
9. Mao, Z.; Anani, A.; White, R. E.; Srinivasan, S.; Appleby, A. J. J Electrochem Soc 1991, 138, 1299–1303.
10. Noringt, J. O. N. E.; Fletchers, E. A. Energy 1982, 7, 651–666.
11. Groisil, M.; Ibrahim, S.; Gupta, A. K.; AlShoaibi, A. Energy Proc. 2015, 75, 3066–3070.
12. Kohl, A.; Nielsen, R. Gas Purification; Gulf Publishing : Houston,TX, 1997.
13. Lawson, J. D.; Garst, A. W. J Chem Eng Data 1976, 21, 20–30.
14. Isaacs, E. E.; Otto, D.; Alan, E. Engineering 1980, 118–120.
15. Lee, J. I. I.; Otto, F. D.; Mather, A. E. J Chem Eng Data 1976, 21, 207–208.
16. Astarita, G.; Savage, D. W.; Bisio, A. Gas Treating with Chemical Solvents; Wiley: New York, 1983.
17. Maity, S. K.; Pradhan, N. C.; Patwardhan, A. V. Appl Catal A: Gen 2006, pp. 251–258.
18. Mandal, B. P.; Biswas, a. K.; Bandyopadhyay, S. S. Sep Purif Technol 2004, 35, 191–202.
19. Xu, H.; Zhang, C.; Zheng, Z. Simulation 2002, 2953–2956.
20. Catino, S. C. Farris, E . Concise Encyclopedia of Chemical Technology; Wiley : New York, 1985.
21. Sakaue, S.; Tsubakino, T.; Nishiyama, Y.; Ishii, Y. J. Org Chem 1993, 58, 3633–3638.
22. Shabbir, H. Gheewala, A. P. A. Water Sci Technol 1997, 36, 53–63.
23. Boon, N.; De Gelder, L.; Lievens, H.; Siciliano, S. D.; Top, E. M.; Verstraete, W. Environ Sci Technol 2002, 36, 4698–4704.
24. Grirrane, A.; Corma, A.; G. H. Science 2008, 322, 1661–1664.
25. Dell'Anna, M. M.; Intini, S.; Romanazzi, G.; Rizzuti, A.; Leonelli, C.; Piccinni, F.; Mastrorilli, P. J MolCatal A: Chem 2014, 395, 307–314.
26. Chen, J.-F.; Jia, T.; Huang, X.-L. Yingyong Huaxue 2000, 17, 672–674.
27. Manieh, A. A.; Sayed, A. Z. Al-Azhar Bull Sci 1995, 6, 35–48.
28. Jessop, P. G.; Ikariya, T.; Noyori, R. Nature 1994, 368, 231–233.
29. Zheng, Y.; Ma, K.; Wang, H.; Sun, X.; Jiang, J.; Wang, C.; Li, R.; Ma, J. Catal Lett 2008, 124, 268–276.
30. Porter, H. K. Org React 2011, 20, 455–481.
31. Setamdideh, D.; Khezri, B.; Mollapour, M. Orient J Chem 2011, 27, 991–996.
32. Gowda, D.; Mahesh, B.; Gowda, S. Indian J Chem 2001, 408, 75–77.
33. Zhao, F.; Fujita, S.; Sun, J.; Ikushima, Y.; Arai, M. Catal Today 2004, 98, 523–528.
34. Liu, S.; Liu, X.; Yu, L.; Liu, Y.; He, H.; Cao, Y. Green Chem. 2014, 4162–4169.
35. Chaudhari, R. V. M.; R. V. Ind Eng Chem Res 1999, 38, 906–915.
36. Huang, J.; Cheng, F.; Binks, B. P.; Yang, H., J Am Chem Soc 2015, 137, 15015–15025.
37. Yang, T.; Wei, L.; Jing, L.; Liang, J.; Zhang, X.; Tang, M.; Monteiro, M. J.; Chen, Y. I.; Wang, Y.; Gu, S.; Zhao,

D.; Yang, H.; Liu, J.; Lu, G. Q. M. Angew Chem int ed. 2017, 56, 8459–8463.
38. Zhang, W.; Fu, L.; Yang, H., ChemSusChem 2014, 7, 391–396.
39. Dauben, W. G. Organic Reactions; Wiley : New York, 1973.
40. Yadav, G. D.; Jadhav, Y. B.; Sengupta, S. J MolCatal A: Chem. 2003, 200, 117–129.
41. Yadav, G. D.; Jadhav, Y. B.; Sengupta, S. Chem Eng Sci 2003, 58, 2681–2689.
42. Yadav, G. D.; Lande, S. V. Ind Eng Chem Res 2007, 46, 2951–2961.
43. Wright, C. Methods for producing aminonitrobenzoic acids, U.S. Patent 8835677 B2, 2014.
44. Starks, C. M. ACS Symposium Series. 1987, 326, 1–7.
45. Maity, S. K.; Pradhan, N. C.; Patwardhan, A. V. Ind Eng Chem Res 2006, 46, 7767–7774.
46. Maity, S. K.; Pradhan, N. C.; Patwardhan, A. V. Chem Eng Sci 2007, 62, 805–813.
47. Yadav, G. D. Top Catal 2004, 29, 145–161.
48. Yadav, G. D.; Naik, S. S. Org Process Res Dev 1999, 3, 83–91.
49. Yadav, G. D.; Naik, S. S. Catal Today 2001, 66, 345–354.
50. Yadav, G. D.; Reddy, C. A. Ind Eng Chem Res 1999, 2245–2253.
51. Yadav, G. D.; Jadhav, Y. B. Langmuir 2002, 18, 5995–6002.
52. Yadav, G. D.; Bisht, P. M. Ind Eng Chem Res 2005, 44, 1273–1283.
53. Yadav, G. D.; Lande, S. V. J Mol Catal A Chem 2006, 244, 271–277.
54. Yadav, G. D.; Lande, S. V. Appl Catal, A: Gen 2005, 287, 267–275.
55. Yadav, G. D.; Lande, S. V. Adv Synth Catal 2005, 347, 1235–1241.
56. Yadav, G. D.; Lande, S. V. J MolCatal A: Chem 2006, 247, 253–259.
57. Scott, W. W. Standard Methods of Chemical Analysis, 6th Edn.; Van Nostrand: New York, 1966.
58. Lin, P.-J.; Yang, H.-M. J MolCatal A: Chem 2005, 235, 293–301.
59. Fujihira T.; Takido, T.; Seno, M. S. J MolCatal A: Chem 1999, 137, 65–75.
60. Gilman, H. Green Syntheses, Wiley: New York, 1941, p. 52.
61. Beutier, D; Renon, H. Ind Eng Chem Process Des Dev 1978, 17, 220–230.
62. Sadegh, N.; Stenby, E. H.; Thomsen, K. Fluid Phase Equilib 2015, 392, 24–32.
63. Maity, S. K.; Pradhan, N. C.; Patwardhan, A. V. Chem Eng J 2008, 141, 187–193.
64. Wang, M. L.; Lee, Z. F. Ind Eng Chem Res 2006, 45, 4918–4926.
65. Wang, M. L.; Tseng, Y. H. J Mol Catal A: Chem 2003, 203, 79–93.
66. Division, E. C. Appl Environ Microbiol 1984, 47, 1295–1298.
67. M. Hojo, Y. Takagi, O, Y. J Am Chem Soc 1960, 82, 2459–2462.